LAWRENCE
LIVERMORE
NATIONAL
LABORATORY

UCRL-PROC-236375

Passive Spectroscopy Bolometers, Grating- And X-Ray Imaging Crystal Spectrometers

M. Bitter, K. W. Hill, S. Scott, S. Paul, A. Ince-Cushmann, M. Reinke, J. Rice, P. Beiersdorfer, M. F. Gu, S. G. Lee, Ch. Broennimann, E. F. Eikenberry

November 8, 2007

Burning Plasma Diagnostics
Varenna, Italy
September 24, 2007 through September 28, 2007

Disclaimer

Passive Spectroscopy Bolometers, Grating- And X-Ray Imaging Crystal Spectrometers

M. Bitter[a], K. W. Hill[a], S. Scott[a], S. Paul[a], A. Ince-Cushman[b], M. Reinke[b], J. E. Rice[b], P. Beiersdorfer[c], M. F. Gu[c], S. G. Lee[d], Ch. Broennimann[e], and E. F. Eikenberry[e]

[a]*Princeton Plasma Physics Laboratory, Princeton, NJ, 08543*
[b]*Plasma Science and Fusion Center, Massachusetts Institute of Technology, Cambridge, MA 02139*
[c]*Lawrence Livermore national Laboratory, Livermore, CA 94550-9234*
[d]*Korea Basic Science Institute, Taejeon 305-333, Korea*
[e]*Paul Scherrer Institut, CH5232 Villigen-PSI, Switzerland*

Abstract: This tutorial gives a brief introduction into passive spectroscopy and describes the working principles of bolometers, a high-resolution grating spectrometer, and a novel X-ray imaging crystal spectrometer, which is of particular interest for profile measurements of the ion temperature and plasma rotation velocity on ITER and future burning plasma experiments.

Keywords: Plasma diagnostic techniques and Instrumentation
PACS: 52.70.Kz, 52.70.La

INTRODUCTION*

Magnetically confined fusion plasmas contain measurable amounts of impurity ions in addition to the hydrogen isotopes which constitute the bulk of the plasma ions. The impurity ions lead to enhanced energy loss and to reduction in the density of the bulk plasma ions, diminishing the fusion reactivity. Spectroscopic measurements of the continuum and line radiation emitted by impurity ions are therefore important to understand and minimize the effects of impurities on plasma performance, but they are also important for the diagnosis of plasma parameters, as e.g. the electron temperature and density, ion temperature, particle transport, and particle influx rates. 'Passive' spectroscopic diagnostics exploit radiation from atomic processes in the plasma, while 'active' spectroscopic diagnostics involve injected particles and laser beams.

The spectral regions of the continuum and line radiation relevant to spectroscopy of tokamak plasmas are defined in Table 1. It is convenient to group the spectroscopic diagnostics by wavelength region and measuring techniques, as they apply to the core and edge of the plasma – see Table 2. In this tutorial, we describe only three passive diagnostic systems: bolometers, a high-resolution grating spectrometer, and a novel x-ray imaging crystal spectrometer. Additional information on passive spectroscopic diagnostics can be found in ref. [1] and the literature cited therein.

TABLE 1: Spectral Regions relevant to Spectroscopy of Tokamak Plasmas

Spectral Region	**Wavelength/Energy Region**
Near Infrared	700-1200 nm / 1-2 eV
Visible	400-700 nm / 2-3 eV
Ultraviolet (UV)	200-400 nm / 3-6 eV
Vacuum Ultraviolet (VUV)	30-200 nm / 6-40 eV
Extreme Ultraviolet (EUV)	10-30 nm / 40-120 eV
Soft X-Ray	0.1-10 nm / 120-12000 eV

TABLE 2: Parameter/Technique for Passive Spectroscopy of Plasma diagnostics

	Impurity species identification	Impurity densities	Z_{eff}	Electron temperature	Ion temperature	Flow velocity	Electron density	Impurity transport	Particle influxes	H/D/T ratio	MHD modes	Runaway electrons	Described in Section
VUV/EUV grating spectroscopy	✸	✸						✸					II.A
VUV/EUV filtered detectors (inc. multilayer mirrors)		✸						✸					II.B&C
Visible bremsstrahlung			✸				❖						II.D
Pulse height analysis	✪	✸	✪	✪									III.B
Filtered SXR diodes		✸						✸			✸		III.C
SXR crystal spectroscopy	❖	✸		❖	✸	✸		❖					IV.B
Edge/divertor visible/UV/near-IR spectroscopy	✪	✸		❖	✸	✸	❖	✸	✸	✸			V.B&C
Visible/UV filtered detectors & filtered cameras		✸		❖			❖	✸	✸				V.D
Fabry-Perot interferometry and visible spectroscopy										✸			V.E
IR synchrotron radiation imaging												✸	VI

✸ Primary (technique is well suited to measurement)
✪ Backup (technique provides useful data but has some limitations compared to primary)
❖ Supplementary (technique provides data that can be used to check or constrain other measurements but is not a reliable measurement itself)

BOLOMETERS

Bolometers monitor the total radiated power from the plasma over a wide spectral range. Compared to grating- and x-ray crystal spectrometers, bolometers have poor spectral resolution, but they are relatively inexpensive and are, therefore, usually implemented in arrays, comprising several detectors, to obtain good spatial coverage. A radial profile of the total radiated power can then be obtained from the data from multiple sightlines by a tomographic reconstruction. Figure 1 shows, as an example, the bolometer array on NSTX. It consists of 16 AXUV-16ELO/G photo-diodes [2], which record the radiation from the plasma through a pinhole from 16 sightlines that are evenly spread over the plasma diameter in the horizontal mid-plane. These diodes have an extremely thin dead layer < 1 μm and, therefore, a high quantum efficiency, near the theoretical limit, for XUV photons from 10 to 8000 eV [2]; and their response is proportional to the photon energy flux.

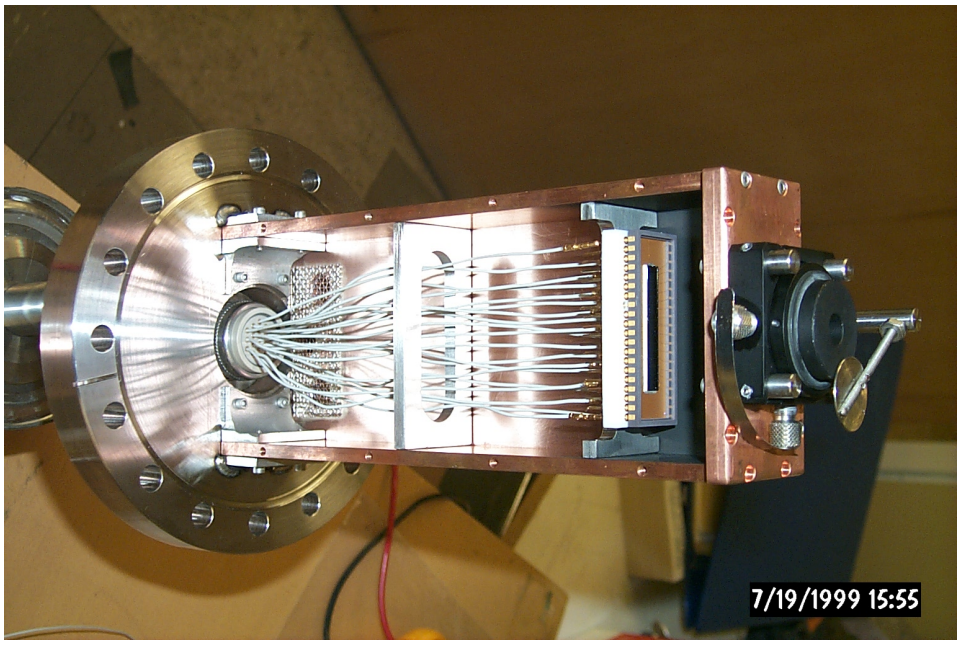

FIGURE 1. Sixteen-channel, horizontally viewing, bolometer on NSTX.

Figure 2 shows the power density profile from a NSTX discharge. The main metallic contributor to the core radiation is iron as seen from XUV spectrometers. An inward impurity pinch led to a central power density of 0.35 Wcm^{-3} and Z_{eff} of 0.6 from metallic contributions. - In addition to AXUV diode arrays [3] many experiments employ foil bolometers [4] which measure the line-integrated power deposited onto a metal foil by observing its resistance change, typically using an AC Wheatstone bridge circuit. This type of detector has a more uniform spectral response than the AXUV diodes but a slower time response and worse signal to noise ratio. More recently, infrared imaging bolometers are being developed for ITER [5].

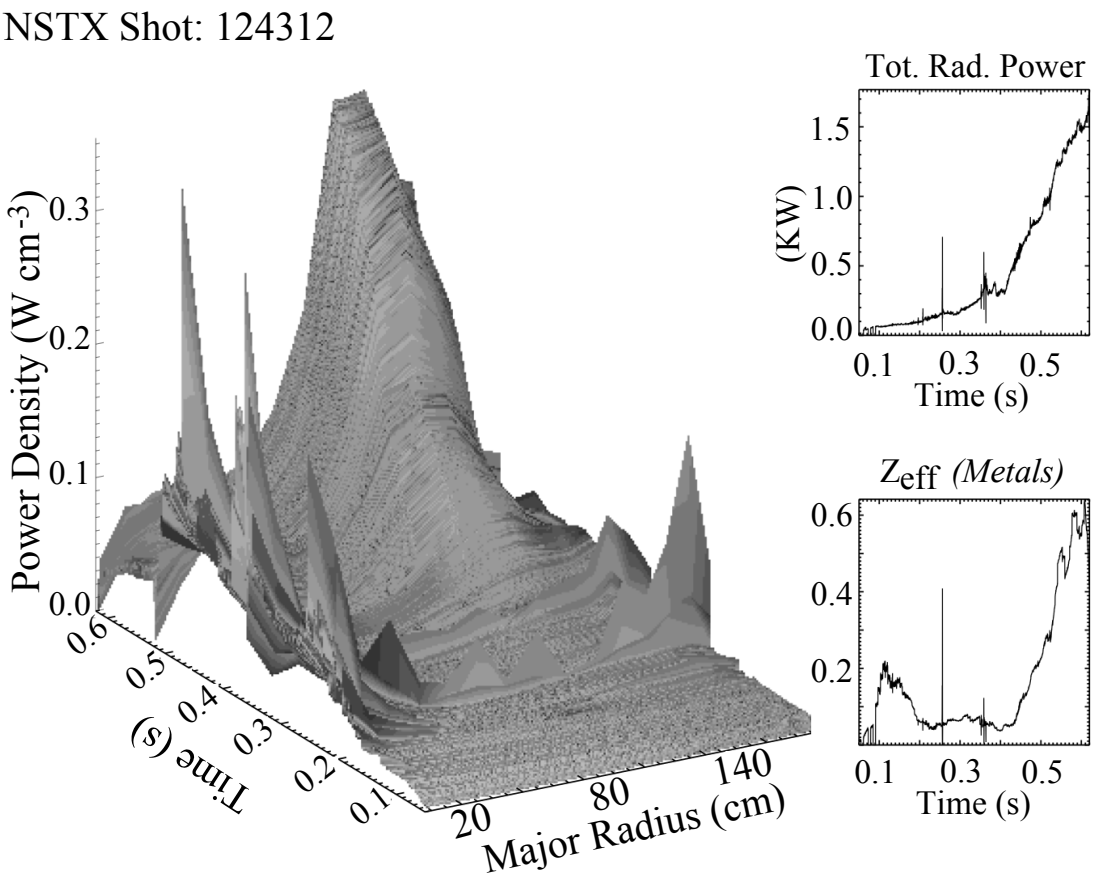

FIGURE 2. Abel-inverted profile of the total radiated power from NSTX

FLAT-FIELD GRATING SPECTROMETERS

A compact grazing-incidence spectrometer has been implemented on NSTX for monitoring impurity line emission in the wavelength range from 6 to 135 Å [6]. This wavelength range is longer than that accessible by a crystal spectrometer [e.g., 7, 8], and shorter than the 100 to 1100 Å range [9, 10], which is covered by the 'Survey, Poor Resolution, Extended Domain (SPRED)' instrument on NSTX. Figure 4 shows the instrument on NSTX, where it was installed at the end of the pump duct. Its line of sight follows a radial line to the center stack of NSTX within the horizontal mid-plane. The instrument is an adaptation of a spectrometer originally used on the Livermore electron beam ion trap [11 - 13]. It employs a variable line spacing grating mounted on a rotary table (average line spacing of 2400 *l*/mm [14]), which affords flat-field focusing with a focal distance of about 23 cm. A 30 μm entrance slit provides a line width of 0.1 Å, i.e., a resolving power of 500 at 50 Å. A 25 mm by 25 mm, liquid nitrogen cooled charge couple device (CCD) camera is used for recording and covers in excess of 50 Å in a single setting. In fast readout mode, the instrument provides a spectrum every 90 ms.

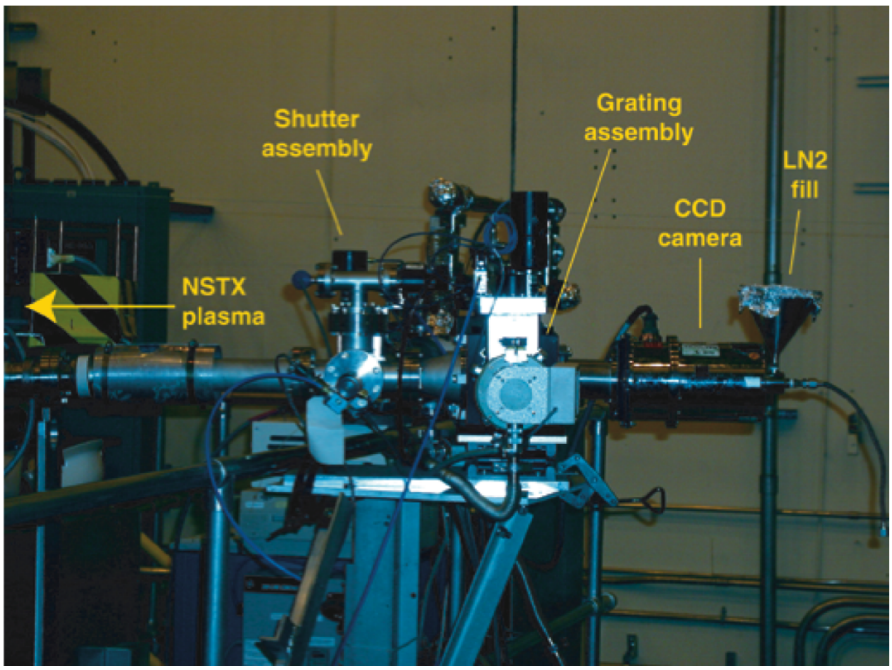

FIGURE 3. Compact grazing-incidence spectrometer on NSTX

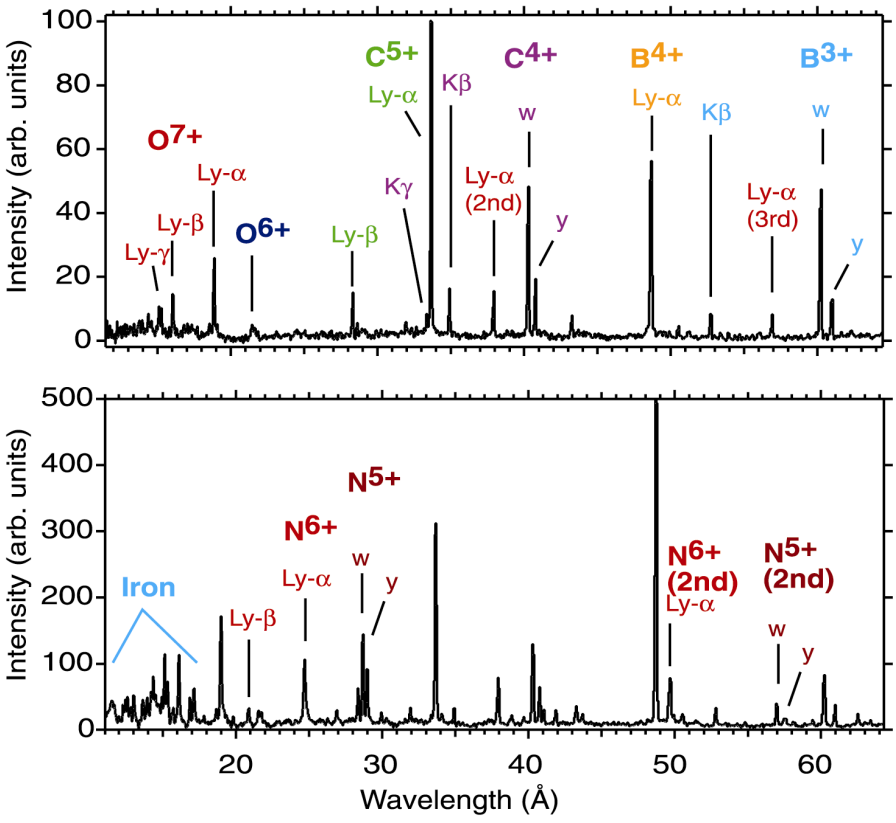

FIGURE 4. Typical K-shell lines and iron L-shell lines (bottom panel)

The instrument typically monitors the emission from hydrogen-like and helium-like boron, carbon, and oxygen, as illustrated in Fig. 4 (top). These three elements are standard impurities in NSTX plasma discharges. Observation of lines from other elements indicates unwanted inflow of impurities from a variety of possible sources. Figure 4 (bottom) shows L-shell lines from iron ions as well as lines from hydrogen-like and helium-like nitrogen entering the plasma during high harmonic fast wave current drive experiments. Other unwanted species detected so far with the grazing-incidence spectrometer include molybdenum, nickel, and titanium.

In some experiments, trace elements have been deliberately introduced into the plasma. For example, argon was injected for ion temperature measurements with the crystal spectrometer; neon was injected for transport measurements using the soft x-ray array; and lithium was evaporated to coat the inner walls. All these elements have been observed with the grazing-incidence spectrometer.

X-RAY IMAGING CRYSTAL SPECTROMETERS

High-resolution x-ray crystal spectrometers have been used for Doppler measurements of the ion temperature and toroidal rotation velocity in the hot core of tokamak plasmas since the 1970's, by analyzing the line spectra from highly charged ions of medium-Z elements from argon to krypton. These elements are present in tokamak plasmas as indigenous impurities, or they are injected for diagnostic purposes. The most commonly used instruments for the x-ray spectroscopy of tokamak plasmas are Johann crystal spectrometers, which consist of a cylindrically bent crystal and a one-dimensional position sensitive detector – see, e.g., Fig. 28 in ref. [1]. The Johann configuration has optimal focusing properties for the so-called meridional rays in the main dispersion plane, perpendicular to the crystal, and it therefore allows the simultaneous observation of an entire spectral range. On the other hand, it does not provide any focusing for the 'sagittal' rays, which are oblique to the main dispersion plane, so that it is not possible to obtain spatially resolved spectra from a tokamak plasma with the standard Johann configuration. This longstanding problem for the x-ray spectroscopy of tokamak plasmas has now been solved by the use of spherically bent crystals, which also provide focusing for the sagittal rays. The concept of these new 'x-ray imaging crystal spectrometers' was described in ref. [15] and then tested on Alcator C-Mod and Textor [16, 17]. These proof-of-principle experiments were, however, conducted with two-dimensional, position-sensitive, multi-wire proportional counters, which had a count rate limit of 400 kHz that was far too low to obtain spectral data with good time resolution and adequate photon statistics. This situation has now changed thanks to the advent of the 'PILATUS II' detector modules, which are pixilated semiconductor diode array of 35 mm x 85 mm with a pixel size of 0.172 mm x 0.172 mm. A PILATUS II detector module consists of a photo-sensitive 'sensor' chip and a sophisticated readout chip that includes an amplifier, comparator, counter, and a memory in each pixel, so that it can handle single photon count rates up to 1 MHz per pixel [18]. Here we present results from a prototype x-ray imaging crystal spectrometer, which has recently been implemented on Alcator C-Mod. The spectrometer consists of two spherically bent (102) quartz

crystals with a 2d-spacing of 4.56216 Å and radii of curvature of 1444 mm and 1385 mm, for observation of He-like and H-like argon at 3.9494 Å and 3.7311 Å, and four PILATUS II detector modules – see Figs. 5 and 6.

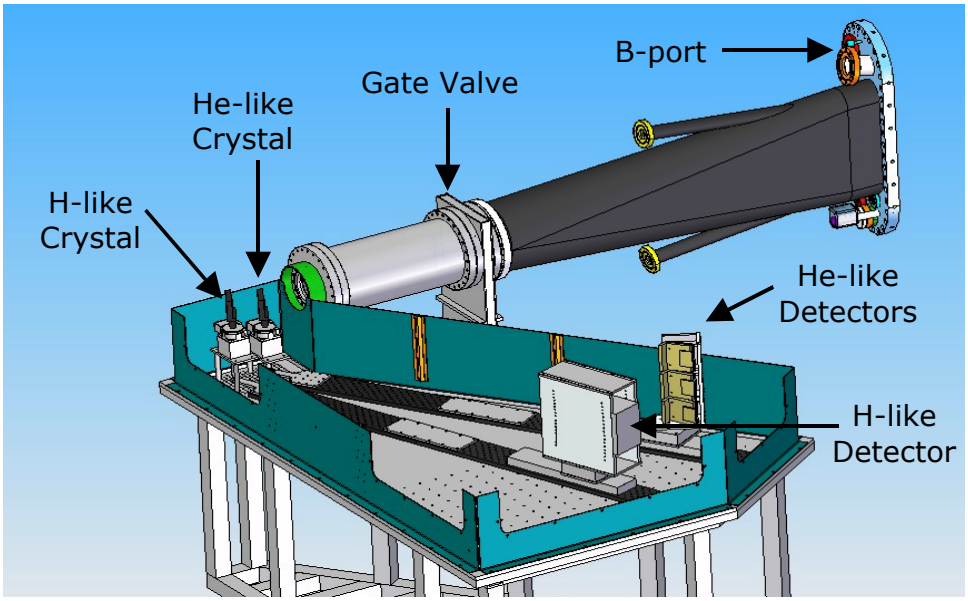

FIGURE 5. Layout of X-ray imaging spectrometer on Alcator C-Mod

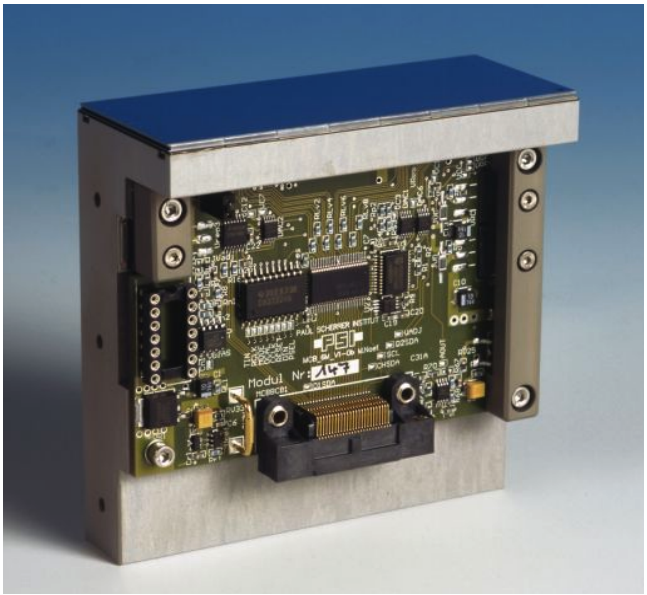

FIGURE 6. PILATUS II detector module

Three PILATUS II detector modules record spatially resolved spectra of He-like argon from the whole, 72 cm high, elongated plasma cross-section, as shown in Fig. 7. The 4th PILATUS II detector module records H-like argon spectra from a 20 cm high, central region of the plasma to allow for reliable measurements of the central ion temperature at high electron temperatures, when the emissivity profile for the He-like argon lines is hollow. Spatially resolved spectra of He-like and H-like argon are now routinely observed on Alcator C-Mod with a time resolution of 20 ms. Figures 8 and 9 show radial profiles of the ion temperature and toroidal plasma rotation velocity as a function of time from the Alcator C-Mod discharge, #1070614011, with a plasma current of 800 kA and auxiliary radio-frequency (rf) heating of 2 MW during the period from 0.7 to 1.2 s. The profiles were constructed from 48 sightlines by dividing the detector in 48 elements in the vertical direction, which corresponds to a spatial resolution in the plasma of 1.3 cm vertically and 1.0 cm radially. The profiles shown in Figs. 8 and 9 represent chord-integrated, non-inverted, data and are, therefore, still preliminary. New software for the inversion of our spectral data is being developed. We note that the central electron temperature during the rf heating phase was 4 keV and that the intensity profile of the (chord-integrated) He-like argon lines was hollow during this period. We can therefore expect that the central values of these profiles will be changed by a final analysis that will be based on the inverted spectral data. We point out that the concept of our x-ray imaging crystal spectrometer has been adopted for the design of the crystal spectrometers for ITER [19] and that the dimensions of the present prototype are quite similar to those of the instruments planned for ITER.

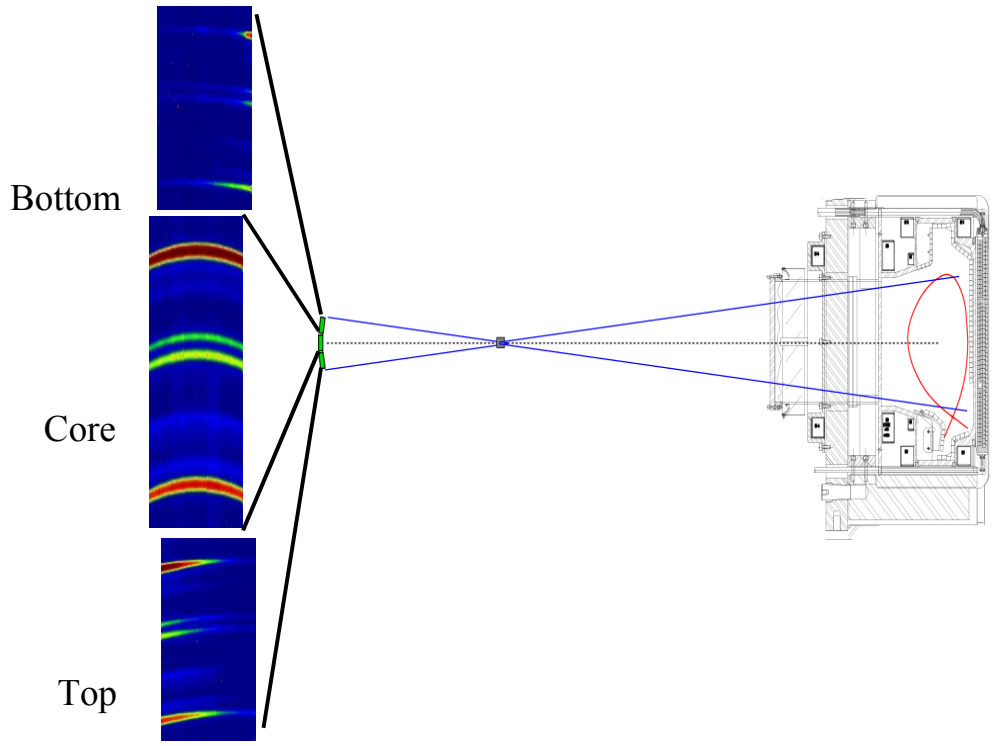

FIGURE 7. Spatially resolved He-like argon spectra from Alcator C-Mod

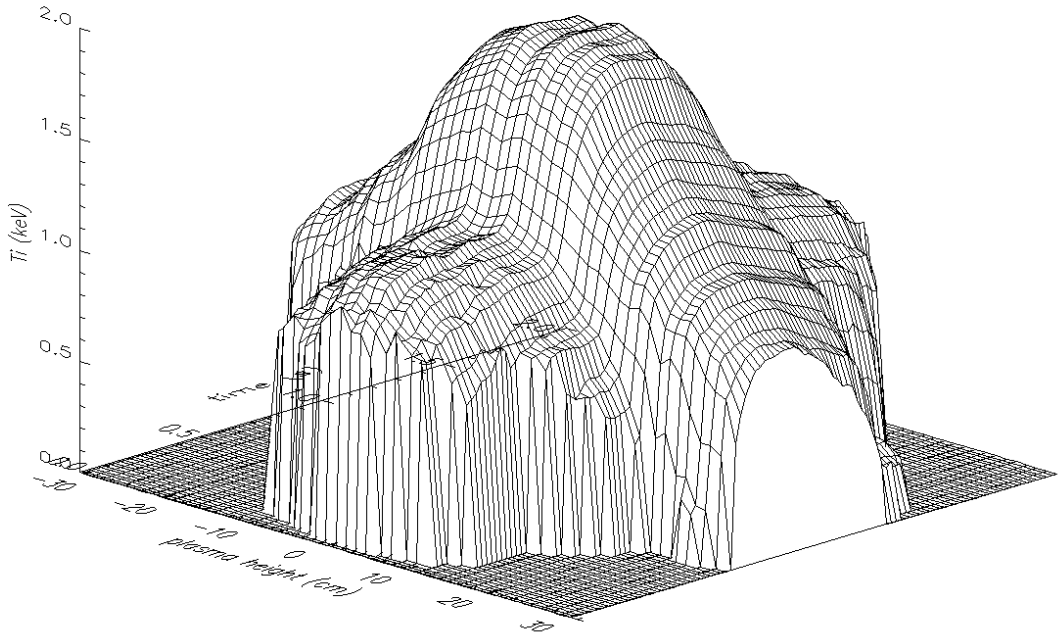

FIGURE 8. Ion-temperature profile as a function of time

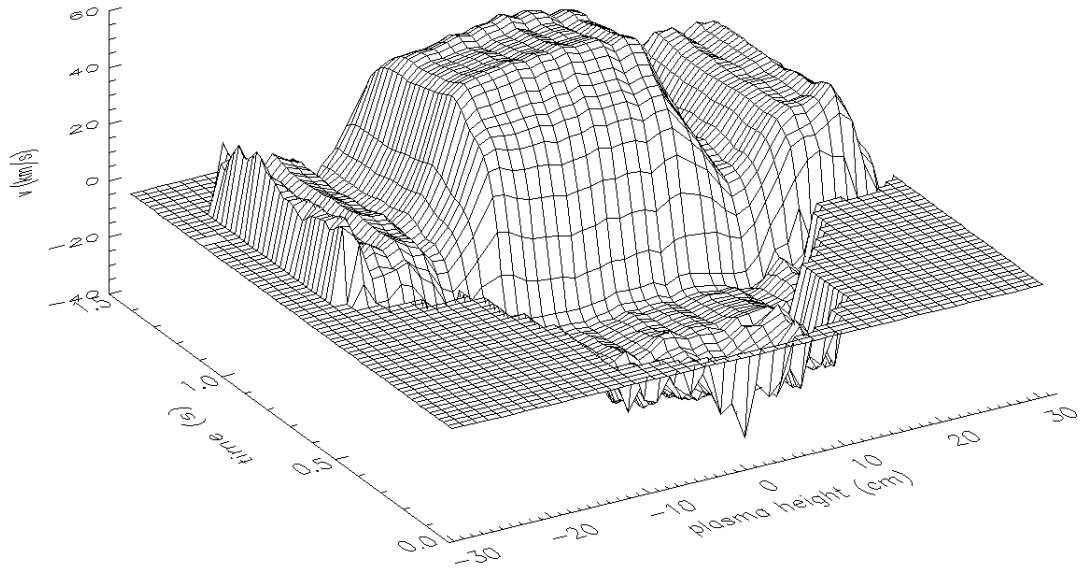

FIGURE 9. Profile of the toroidal rotation velocity as a function of time

CONCLUSIONS

'Passive' spectroscopic diagnostics play an important role in determining effects of impurities and in measurements of plasma parameters. The diagnostic techniques are being continuously improved to obtain better spatial and time resolution and to meet the requirements for burning plasma experiments. New developments in x-ray spectroscopy may lead to an attractive alternative to 'active' spectroscopic diagnostics, such as the challenging beam-based charge-exchange recombination spectroscopy, for the measurements of ion-temperature and plasma rotation velocity profiles in those experiments.

ACKNOWLEDGEMENTS

We gratefully acknowledge the support of our work by the US Department of Energy (DOE) through Contracts No. DE-AC02-76CHO3073, No. DE-AC52-07NA27344, and No. DE-FC02-99ER54572 with the Princeton Plasma Physics Laboratory, the Lawrence Livermore National Laboratory, and the Plasma Science & Fusion Center at the Massachusetts Institute of Technology. We also gratefully acknowledge the funding of our project by the DOE Diagnostics Development Initiative under the direction of Darlene Markevich.

REFERENCES

*This introduction is drawn from ref. [1].

1. B. C. Stratton, M. Bitter, K. W. Hill, D. L. Hillis, and J. T. Hogan, *'Passive Spectroscopic Diagnostics for Magnetically-Confined Fusion Plasmas',* to be published in the February 2008 issue of Fusion Science and Technology,
2. http://www.ird-inc.com/axuvarr.html
3. R. L. Boivin, et al., *Rev. Sci. Instrum. **70**, 260 (1999)*
4. K. F. Mast, et al., *Rev. Sci. Instrum. **62**, 744 (1991)*
5 G. A. Wuerden and B. J. Peterson, *Rev. Sci. Instrum. **70**, 255 (1999)*
6. P. Beiersdorfer, et al., *Rev. Sci. Instrum.* **77**, 10F306 (2006).
7. P. Beiersdorfer, et al., *Rev. Sci. Instrum.* **77**, 1974 (2003).
8. P. Beiersdorfer, et al. *Rev. Sci. Instrum.* **60**, 895 (1989).
9. R. J. Fonck, et al., Appl. Optics **21**, 2115 (1982).
10. B. C. Stratton, et al., *Rev. Sci. Instrum.* **57**, 2043 (1986).
11. S. B. Utter, et al., *Rev. Sci. Instrum*. **70**, 284 (1999).
12. P. Beiersdorfer, et al., *Rev. Sci. Instrum.* **70**, 276 (1999).
13. A. T. Graf, *et al.*, *Can. J. Phys.* (in press).
14. N. Nakano, et al., *Appl. Optics* **23**, 2386 (1984).
15. M. Bitter, *et al.*, *Rev. Sci. Instrum.* **70**, 292 (1999).
16. M. Bitter, *et al.*, *Rev. Sci. Instrum.* **75**, 3660 (2004).
17. G. Bertschinger, *et al.*, *33rd EPS Conference Rome, 2006*, vol. 30I, P-2.153.
18. http://pilatus.web.psi.ch/pilatus.htm
19. R. Barnsley, et al., *Rev. Sci. Instrum. **75**, 3743 (2004)*